The two-layer conceptual model of hard-rock aquifers: validation with a deterministic hydrogeological model

Le modèle conceptuel bicouche des aquifères de socle : validation avec un modèle hydrogéologique déterministe

Durand V.[(1)], Léonardi V.[(2)], de Marsily G.[(3)], Lachassagne P.[(4)]

(1) UMR 8148 GEOPS, Univ. Paris Sud, 91405 Orsay Cedex; CNRS; veronique.durand@u-psud.fr

(2) Hydrosciences Montpellier, UMR 5569, Univ. de Montpellier; veronique.leonardi@um2.fr

(3) Sorbonne Universités, UPMC Univ. Paris 06; CNRS; EPHE; UMR 7619 Metis; 4 place Jussieu, 75005 PARIS, gdemarsily@aol.com

(4) Danone Waters, Evian-Volvic-World, BP 87, 74500 Evian-les-Bains Cedex; patrick.lachassagne@danone.com

I. Introduction

Hard-Rock (HR) aquifers have long been considered as two-layer systems, with a mostly capacitive layer just below the surface, the weathered layer, and a mostly transmissive layer underneath, the fissured layer, both belonging to the HR weathering profile. Although this hydrogeological conceptual model now gathers a large consensus in the scientific community (Lenck, 1977 ; Rushton, 1986 ; Detay et al., 1989 ; Howard and Karundu, 1992 ; Maréchal et al., 2004 ; Dewandel et al., 2006 ; Lachassagne et al., 2011), it is difficult to prove that it can be efficient in terms of deterministic modeling, especially with an equivalent porous medium model for the fissured aquifer (Gupta et al., 1985 ; Engerrand, 2002), which would not be the first choice for "fractured aquifers" (Cacas et al., 1990 ; Banwart et al., 1994 ; Le Borgne et al., 2004 ; Ahmed et al., 2008). To our knowledge, these models always consider only one layer for simplicity reasons and it has never been demonstrated that a two-layer model can be more efficient than a single-layer one. Consequently, the objectives of this presentation are to present a new methodology developed for the calibration of such a two-layer finite-difference hydrogeological model and to show that it enables to identify and efficiently calibrate, in transient state, the hydrodynamic parameters of each of the two layers.

II. Study site and methodology

II. 1 Study site

The studied site (Durand et al., 2006) is located in north-west Brittany, France, 10 km from the English Channel shoreline (Fig. 1), in a landscape of grass-land, forest and farmland, with a smooth relief. In an area covering only 4 km², six pumping wells and 40 boreholes, owned and surveyed by the Nestlé Waters Company for bottled natural mineral and spring water, provide an unusually rich set of hydrogeological data. In the middle of the studied site stands a 90 m asl hill, surrounded by the Arguenon River at 10 m asl flowing toward the English Channel (Fig. 1). The migmatites that constitute the rocks in this area belong to the Saint-Malo dome, exhumed at the end of the Cadomian Orogeny (540 Ma). These partially melted rocks originated from detrital sediments interbedded with graphitic cherts, composed of quartz. They now form a folded gneiss matrix with relic bands of cherts. They were later intruded by dolerite dykes during the Hercynian period (330 Ma). The associated hard-rock aquifer is mostly located in the sub-surface stratiform weathered layers (Durand et al., 2006), which consist of: (i) a cover of unconsolidated weathered rocks, several tens of meters thick when it is preserved from erosion, mainly consisting of clays or sandy clays, which are the weakly permeable transformation products of the initial minerals; (ii) beneath this layer, and above the unweathered bedrock, a fissured zone, some 50 m thick or more, resulting from rock shattering under the influence of stress generated by the swelling of certain minerals during the early stages of weathering (Lachassagne et al., 2001 ; Wyns et al., 2004 ; Dewandel et al., 2006 ; Lachassagne et al., 2011). Field surveys and geophysical mapping of the two weathered layers and of the various geological heterogeneities, such as graphitic cherts, dolerite dykes and fractures, have been reported in a previous study (Durand et al., 2006).

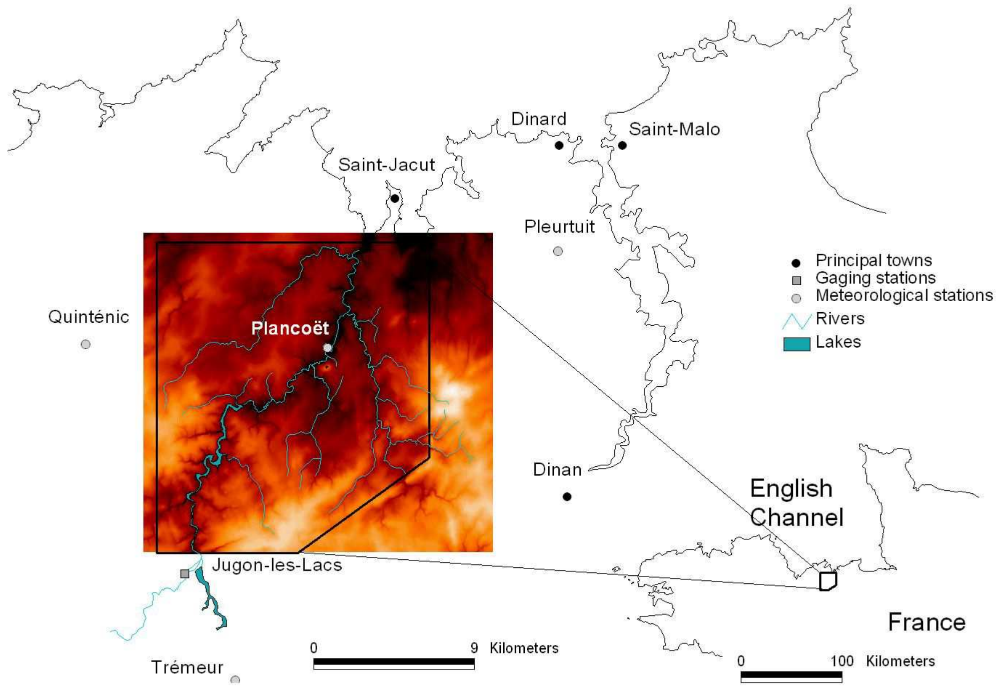

Figure 1 – Location and Digital Elevation Model of the study area (within the black frame), the three used meteorological stations, and the used gauging station

II. 2 Model description

The finite-difference PMWIN model (Chiang and Kinzelbach, 2000) that uses the MODFLOW code (Harbaugh and McDonald, 1996) has been chosen for this work. The model was built with two parallel layers simulating the assumed different hydrodynamic properties of both the weathered layer (layer 1), and the underlying weathered fissured layer (layer 2). The geometry of each of these layers (shape of top and bottom) was determined by extensive field work over the total 116 km² studied area (Durand et al., 2006). The maximum thickness of layer 2, when totally preserved from erosion, was considered as constant over the studied area and was estimated at 100 m, a thickness consistent with our experience of the Brittany geological context and the available geological and geophysical data. Layer 2 is present over the whole modeled area (116 km²), as it has not been totally eroded, whilst layer 1 covers only 54 km², due to local areas of total erosion (Fig. 1); its maximum thickness is 40 m. In the central zone of the modeled area, owned by Nestlé Waters, the accuracy of the structural map and the number of hydrogeological data are much higher than in the other areas, close to the bottled water exploitation zone. The rectangular grid size is therefore a compromise between a good precision where the data are dense and relatively fast calculations: the width of the rectangular model cells varies from 400 m on the borders to 40 m in the exploitation zone (Fig. 2). Each of the two layers is modeled vertically by a single cell whose height is equal to the thickness of the corresponding layer. The layers are vertically connected, as they are assumed to be in reality. Layer 1 is modeled as unconfined and layer 2 can be either confined or unconfined, depending on the presence of a confining layer (bottom of layer 1) through which leakage can occur, and on the potential lowering of the piezometric head below the elevation of this confining layer.

The simulations were performed under a transient flow regime which allowed the time-dependent seasonal and yearly piezometric variations observed in the aquifer to be reproduced. The modeling runs from 1/1/1996 to 30/11/2003, with a time step of 15 days, similar to the frequency of piezometric measurements. The daily rainfall data were measured directly at the bottling plant; three weather stations belonging to Météo France around Plancoët, located in Pleurtuit, Quinténic and Trémeur (Fig. 1), also provided data on rainfall and daily potential evapotranspiration (ET) estimated with Penman's equation (Penman, 1948). River flow measurements were available at the Jugon-les-Lacs gauging station (Fig. 1) located on the Arguenon River, which drains the studied area, to the south. The meteorological daily data of the near-by Trémeur station were used to calibrate the soil maximum storage capacity (called RFU) in order to fit the river discharge with Thornthwaite's approach. The daily rainfall water is stored in the soil reservoir until the RFU is reached. The daily potential ET is subtracted from this reservoir if it contains enough water. The actual daily ET is then equal to the potential ET. If not, the actual daily ET is equal to the available water in the reservoir. When the soil reservoir is full and the actual ET equals the potential ET, the additional daily rainwater is the effective rainfall (Eff_R). The value of RFU that best matches our estimate of annual effective rainfall, which is on average of 247 mm/y, derived from the annual specific flow of the river, is 100 mm. In this hydrogeological context, both runoff and recharge are assumed to reach the river. To calibrate RFU, the rainfall data of the Plancoët station were used together with the ET weighted average of the three meteorological stations, which is justified by the similarity between the weighted average rainfall and the Plancoët local rainfall data. In the hydrogeological model, various recharge hypotheses were tested, based on various proportions of the time-variant effective rainfall assigned to recharge or to runoff.

Six pumping wells in the exploitation zone (Fig. 2) are used for bottled water production and their time-varying discharges are precisely recorded by Nestlé Waters. No other significant pumping is known in the whole modeled domain, other than a few tens of liters per day in summer from the shallow wells of some houses, not considered in this study. The total modeled domain, chosen much larger than the area exploited by the bottling plant, is limited by rivers, considered as constant head boundaries (Fig. 2). The river elevations were extracted from the 1/25 000 topographic map of the area (IGN, 2000) assuming a linear slope between known points. In the exploitation zone, the topographic depression resulting from a disused quarry of graphitic cherts located near the top of a hill is at the origin of a perennial small lake. The level of this lake, most of the time higher than the observed nearby piezometric levels, shows that it functions as an infiltration zone. It is modeled as a reservoir in the MODFLOW code (Fig. 2), with a prescribed constant level, a water depth of 1 m, and an underlying 1 m-thick sediment layer with a vertical hydraulic conductivity of 1 m/d ($1.2\ 10^{-5}$ m/s). This value was calibrated so that the infiltration from the lake is consistent with its hydrological balance. Two small temporary rivers (Fig. 2) surrounding the hill are considered as drains in the model, because they drain the aquifer during high water periods and are dry during the rest of the year. A calibrated hydraulic conductance of 50 m^2/d ($5.8\ 10^{-4}$ m^2/s) was assigned to them. The initial value of the piezometric heads on 1/1/1996 was estimated as follows: a preliminary run over the whole 8 year period started with heads at the ground surface; the calculated heads on 30/11/2003 at the end of this preliminary run were then taken as the initial conditions.

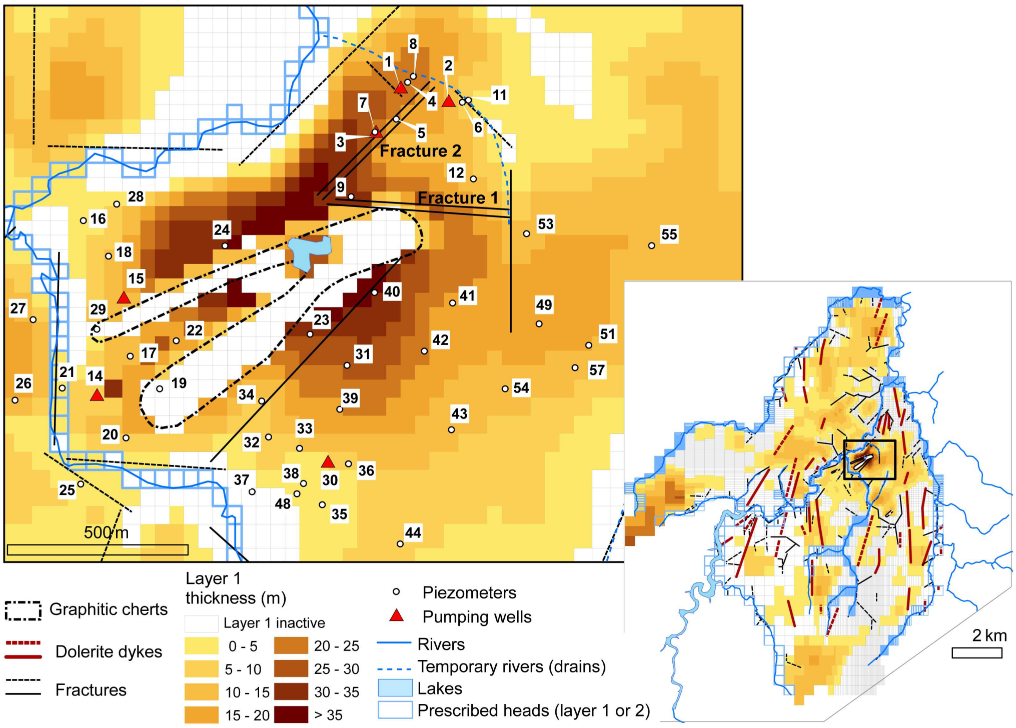

Figure 2 – Geometry of the finite-difference model, boundary conditions, thickness of layer 1 (white color means zero thickness) and location of the geological heterogeneities

II. 3 Calibration approach

The main difficulty of the calibration process is to insure the consistency between the aquifer hydrodynamic parameters on the one hand, and the total flow through the aquifer, i.e. the recharge, on the other hand. In order to overcome this problem, a large number of parameter sets have been tested. At first, it was considered that the hydraulic conductivity could be very heterogeneous in this type of aquifer, and that the heterogeneity would not depend primarily on the two-layer model, but more on the location of fractures and other spatial discontinuities. As this type of heterogeneities was not the main interest here, a homogeneous hydraulic conductivity for both layers was chosen, using the PEST automatic calibration method to give the best possible average fit. Fixing the recharge to 100% Eff_R, and calibrating simultaneously the hydraulic conductivity and the specific yield, both homogeneous in space and identical for the two layers, the best calibrated hydraulic conductivity was 0.07 m/d (8.1 10^{-7} m/s), and the specific yield was 6 %.

The hydraulic parameter that could be considered as the most representative for the two-layer model was the specific yield (Sy), also called the storage capacity. Contrary to the hydraulic conductivity, which influences the average hydraulic heads, this parameter influences the amplitude of the hydraulic head variations. The piezometric signals in this type of aquifer in a temperate climate present indeed a sinusoidal shape with an annual period, the highest levels being at the end of winter, and the lowest levels at the end of summer. The amplitude of the head variation between the high and low levels depends upon both the time distribution of the recharge and the Sy values. As the specific yield is a parameter that has an active role for an unconfined layer only, it is either Sy in layer 1 (Sy1) or Sy in layer 2 (Sy2) that is effective, depending on the piezometer location: Sy1 will be effective where layer 1 (weathered layer) is present and saturated, and Sy2 will be effective where layer 1 has been eroded or is dry. In the data set, both piezometer types are well represented, and it is interesting to compare the signals obtained for each type. To manage the interdependency between the recharge, Sy1 and Sy2, the sensitivity of the hydraulic heads to these three parameters was analyzed through a large number of model parameter sets: eight values for each parameter were selected (Recharge - "Rech" - from 30 to 100 % of Eff_R, Sy1 and Sy2 from 1 to 10%), and the whole set of the 512 (8^3) resulting models was run.

In order to quantify the quality of fit for each model, the classical head squared deviation variance (Var) between the calculated and observed heads was calculated for all piezometers. It appeared however that this criterion was not very efficient to measure the quality of the amplitude variation of the simulation signals. To better fit the recharge and the specific yield, a new quality-of-fit criterion, "Advar", was developed, based on the seasonal piezometric amplitude variation. For each piezometer, and for each available measurement at a time j, a moving interval of one year after j was defined both for the observed and the calculated heads. Then for that one-year interval, each piezometer punctual amplitude-deviation variance Advar is defined as the average of the amplitude squared deviation (Equation 1):

$$\mathrm{Advar} = \frac{\sum_{d=1}^{n_{year}} \left[\left(\max_{calc_d} - \min_{calc_d}\right) - \left(\max_{obs_d} - \min_{obs_d}\right)\right]^2}{n_{day}} \qquad (1)$$

with $\max_{calcd}$, $\min_{calcd}$, $\max_{obsd}$, $\min_{obsd}$ respectively the maximum-minimum values of the calculated and observed heads over the one-year interval after the date d, and n_{day} the number of measurement dates j available, i.e. the total number of data points less those of the last year of data. The total average over the 40 piezometers was calculated for each model. Like the variance, Advar is always positive and the smaller values indicate a better model fit.

III. Results and discussion

The results of the average quality-of-fit criteria (average for the 40 boreholes) are presented in an exhaustive manner: on Figure 3 and 4, one can see the evolution of Var (first line) and Advar (second line) as a function of Rech (Figure 3) or Sy2 (Figure 4). Each column corresponds to a distinct value of Sy1, and each curve to a distinct value of Sy2 (Figure 3) or Rech (Figure 4). The scale of the Y axis is identical for all Var, but the scale has been changed for Advar between Sy1=3 % and Sy1= 4%, in order to observe the large variations of this criterion.

One can first notice that the lowest Var and Advar values are mostly obtained for the highest recharge parameter. For Var, the curve shapes on Figure 3 are very similar, showing a general better fit towards the high recharge values, and a lower Var for the highest Sy2. For Sy1 up to 3 %, the best fit is obtained for a recharge of 100 % Eff_R, and for higher Sy1 values, this recharge is less effective and varies between 80 and 100 % Eff_R. For Advar, the analysis is more delicate, as the Sy2 curves on Figure 3 do not show a homogeneous behaviour. For Sy1 up to 3 %, the lowest Advar values are obtained for the lowest recharge. On the contrary, when Sy1 increases, except for the lowest Sy2 values, most of the lowest Advar values are obtained with the maximum recharge, and here the difference between 80, 90 and 100 % Eff_R is more sensitive than for Var. This leads to conclude that the recharge for this aquifer is equal to the effective rainfall, implying that runoff is negligible. Considering the landscape with smooth relief and grassy hills, this seems realistic. Previous estimations made elsewhere in Brittany (Merot et al., 1981 ; Durand and Juan Torres, 1996 ; Molénat et al., 1999) by other methods such as isotope analysis or river discharge recessing analysis came to similar conclusions.

Figure 4 shows distinct behaviours for Var and Advar as a function of Sy2. Looking at the Var criterion only, one could conclude that the best fit would be obtained with the highest values of Sy2, even above 10 %, which is not realistic for such a hydrogeological context. We found the same result with PEST, the highest potential values were obtained for Sy2. Looking at the Advar criterion however, the best fit for Sy2 is between 4 and 6 %, which, even quite high for a fissured layer, is more realistic.

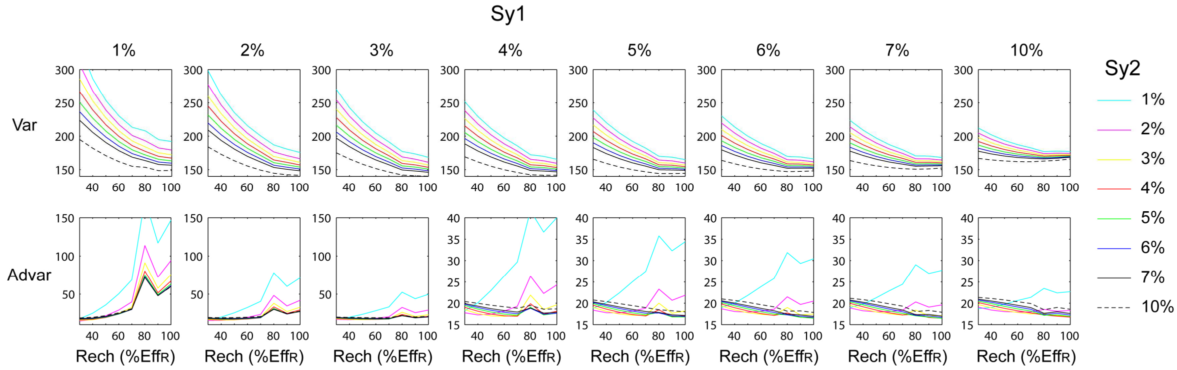

Figure 3 – Results of the quality criteria Var and Advar as a function of the recharge values on the X axis, each curve representing a distinct Sy2 value, and each column a distinct Sy1 value

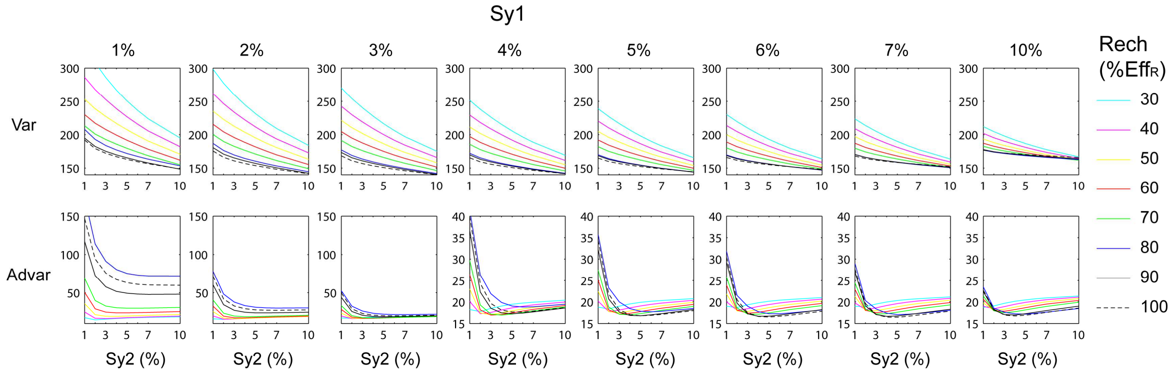

Figure 4 – Results of the quality criteria Var and Advar as a function of the Sy2 values on the X axis, each curve representing a distinct recharge value, and each column a distinct Sy1 value

Another way of presenting the results obtained for the various Sy is in matrices: in Table 1, the values of Var and Advar obtained with the maximum recharge are arranged in tables with distinct Sy1 values in columns and Sy2 values in rows. The minimum Var and Advar values are highlighted in color. One can notice that the colored cells are below the diagonal matrix, ie for Sy2>Sy1, with Var, and above the diagonal matrix, ie for Sy1>Sy2, with Advar. This shows that the weathered layer is indeed more capacitive than the fissured layer, as written in the literature (e.g. Wyns et al., 2004), and that these properties can be demonstrated by modelling with a two-layer finite difference model.

These results are consistent with the conceptual model developed by Lachassagne et al. (2001), notably with a decrease of Sy with depth. The obtained Sy values (6%<Sy1<7% and 4%<Sy2<5% for the best Advar values) are higher than those given by Rushton and Weller (1985) for an Indian granite and by Compaore et al. (1997) for a granitic massif in Burkina Faso, who estimated the specific yield of the weathered zone between 1 and 2%. Nevertheless, as shown by Wyns et al. (2004), Sy in the weathered (layer 1) is sensitive to the type of lithology: for instance Sy increases with the coarsening of the minerals constituting the parent rock and also increases with the quartz content. The interval of specific yield values measured by Wyns et al. (2004) on several different types of lithologies in French Britanny includes the estimated values in the present study.

IV. Conclusion

This paper leads to conclude on tree distinct points. First, the runoff has been found to be negligible on this site. Second, a new quality-of-fit, Advar, has been developed, based on the seasonal amplitude variations, and it helps to calibrate the specific yield, impossible with the Var classical criterion. And third, the weathered layer seems here a little more capacitive than the fissured layer: this could be shown with the help of a two-layer deterministic hydrogeological model and the new Advar criterion.

		Sy1							
		1%	2%	3%	4%	5%	6%	7%	10%
Sy2	1%	192	176	168	165	165	166	168	177
	2%	179	166	161	159	160	162	164	174
	3%	172	161	157	156	157	159	162	173
	4%	167	157	154	153	154	157	160	171
	5%	163	154	151	151	152	155	159	170
	6%	160	151	148	149	151	154	157	169
	7%	157	148	146	147	149	152	156	168
	10%	149	142	140	142	144	148	152	166

Var

		Sy1							
		1%	2%	3%	4%	5%	6%	7%	10%
Sy2	1%	146.7	71.4	49.7	40.0	34.4	30.4	27.7	22.7
	2%	94.2	41.9	29.1	24.3	21.9	20.5	19.6	18.3
	3%	75.7	32.7	23.0	19.6	18.2	17.5	17.1	16.9
	4%	67.2	29.2	20.8	18.1	17.1	16.6	16.5	16.8
	5%	63.0	27.7	20.1	17.7	16.8	16.5	16.5	16.9
	6%	61.1	27.3	19.9	17.7	16.9	16.7	16.7	17.2
	7%	60.2	27.2	20.1	17.9	17.1	16.9	17.0	17.6
	10%	59.7	27.7	20.8	18.7	18.0	17.8	17.9	18.6

Advar

Table 1 – Var and Advar values obtained with the maximum recharge for all Sy1 and Sy2 values. In yellow: minimum values; in orange, red and brown red respectively: classes around the minimum, adding successively either 5% (for Var) or 0.2% (for Advar) of the total variation range

Aknowlegdment

We are grateful to the Nestlé Waters Company for financial support and for making the data available.

References

Ahmed S., Maréchal J.-C., Ledoux E. and de Marsily G. (2008). - Groundwater modelling in hard-rock terrain in semi-arid areas: experience from India. *In: Hydrological Modelling in Arid and Semi-Arid Areas*, *Wheater, Sorooshian and Sharma Eds. Cambridge, UK*, *Cambridge University Press, 157-189*.

Banwart S., Gustafsson E., Laaksoharju M., Nilsson A. C., Tullborg E. L. and Wallin B. (1994). - Large-Scale Intrusion Of Shallow-Water Into A Vertical Fracture-Zone In Crystalline Bedrock - Initial Hydrochemical Perturbation During Tunnel Construction At The Aspo-Hard-Rock-Laboratory, Southeastern Sweden. *Water Resources Research*, *30 (6), 1747-1763.*

Cacas M.-C., Ledoux E., de Marsily G., Tillie B., Barbreau A., Durand E., Feuga B. and Peaudecerf P. (1990). - Modeling fracture flow with a discrete fracture network: calibration and validation - 1. The flow model. *Water Resources Research*, *26 (3), 479-489.*

Chiang W. H. and Kinzelbach W. (2000). - 3D-Groundwater Modeling with PMWIN – A Simulation System for Modeling Groundwater Flow and Pollution. *Springer-Verlag Berlin Heidelberg New York*, *346*.

Compaore G., Lachassagne P., Pointet T. and Travi Y. (1997). - Evaluation du stock d'eau des altérites. Expérimentation sur le site granitique de Sanon (Burkina-Faso). *Hard Rock Hydrosystems*, *Rabat*, *IAHS, 241, 37-46.*

Detay M., Poyet P., Emsellem Y., Bernardi A. and Aubrac G. (1989). - Influence du développement du réservoir capacitif d'altérites et de son état de saturation sur les caractéristiques hydrodynamiques des forages en zone de socle cristallin. *Comptes rendus de l'Académie des Sciences de Paris, Série II a*, *309*, *429-436*.

Dewandel B., Lachassagne P., Wyns R., Maréchal J.-C. and Krishnamurthy N. S. (2006). - A generalized 3-D geological and hydrogeological conceptual model of granite aquifers controlled by single or multiphase weathering. *Journal of Hydrology*, *330 (1-2), 260-284.*

Durand P. and Juan Torres J. L. (1996). - Solute transfer in agricultural catchments: the interest and limits of mixing models. *Journal of Hydrology*, *181*, *1-22*.

Durand V., Deffontaines B., Léonardi V., Guérin R., Wyns R., de Marsily G. and Bonjour J.-L. (2006). - A multidisciplinary approach to determine the structural geometry of hard-rock aquifers. Application to the Plancoët migmatitic aquifer (NE Brittany, W France). *Bulletin de la Société Géologique de France*, *177 (5)*, *227-237*.

Engerrand C. (2002). - Hydrogeology of the weathered-fissured hard rock aquifers located in monsoon areas: hydrogeological study of two watersheds in Andhra Pradesh (India). *Thèse Université Paris 6*, *Paris*, *203 p.*

Gupta C. P., Thangarajan M. and Gurunadha Rao V. V. S. (1985). - Evolution of regional hydrogeologic setup of a hard rock aquifer through R-C analog model. *Ground Water*, *23 (3)*, *331-335*.

Harbaugh A. W. and McDonald M. G. (1996). - User's documentation for MODFLOW-96, an update to the U.S. Geological Survey modular finite-difference ground-water flow model. *Open-File Report, USGS, 96-485, 56 p.*

Howard K. W. F. and Karundu J. (1992). - Constraints on the exploitation of basement aquifers in East Africa. Water balance implications and the role of the regolith. *Journal of Hydrology*, *139*, *183-196*.

IGN (2000). - TOP25 1016ET, Saint-Cast-le Guildo/Cap Fréhel (GPS).

Lachassagne P., Wyns R., Bérard P., Bruel T., Chéry L., Coutand T., Desprats J.-F. and Le Strat P. (2001). - Exploitation of high-yields in hard-rock aquifers: downscaling methodology combining GIS and multicriteria analysis to delineate field prospecting zones. *Ground Water*, *39 (4)*, *568-581*.

Lachassagne P., Wyns R. and Dewandel B. (2011). - The fracture permeability of hard rock aquifers is due neither to tectonics, nor to unloading, but to weathering processes. *Terra Nova*, *23*, *145-161*.

Le Borgne T., Bour O., Dreuzy J. R. d., Davy P. and Touchard F. (2004). - Equivalent mean flow models for fractured aquifers: insights from a pumping tests scaling interpretation. *Water Resources Research*, *40 (3)*, *W03512*.

Lenck P.-P. (1977). - Données nouvelles sur l'hydrogéologie des régions à substratum métamorphique ou éruptif. Enseignements tirés de la réalisation de 900 forages en Côte-d'Ivoire. *Comptes rendus de l'Académie des Sciences de Paris, Série II a*, *285*, *497-500*.

Maréchal J.-C., Dewandel B. and Subrahmanyam K. (2004). - Use of hydraulic tests at different scales to characterize fracture network properties in the weathered-fractured layer of a hard rock aquifer. *Water Resources Research*, *40 (11)*, *W11508*.

Merot P., Bourguet M. and Le Leuch M. (1981). - Analyse d'une crue à l'aide du traçage naturel par l'oxygène 18 mesuré dans les pluies, le sol, le ruisseau. *CATENA*, *8 (1)*, *69-81*.

Molénat J., Davy P., Gascuel-Odoux C. and Durand P. (1999). - Study of three subsurface hydrologic systems based on spectral and cross-spectral analysis of time series. *Journal of Hydrology*, *222*, *152-164*.

Rushton K. R. (1986). - Vertical flow in heavily exploited hard rock and alluvial aquifers. *Ground Water*, *24 (5)*, *601-608*.

Rushton K. R. and Weller J. (1985). - Response to pumping of a weathered-fractured granite aquifer. *Journal of Hydrology*, *80*, *299-309*.

Wyns R., Baltassat J.-M., Lachassagne P., Legtchenko A., Vairon J. and Mathieu F. (2004). - Application of Proton Magnetic Resonance Soundings to groundwater reserve mapping in weathered basement rocks (Brittany, France). *Bulletin de la Société Géologique de France*, *175 (1)*, *21-34*.